

## WAVELET BASED FILTERS FOR ENHANCING DIGITAL MAMMOGRAMS

Emmanouil Athanasiadis<sup>1</sup>, Nikos Piliouras<sup>2</sup>, Dimitris Glotsos<sup>1</sup>, Ioannis Kalatzis<sup>2</sup>, Nikos Dimitropoulos<sup>3</sup>,  
and Dionisis Cavouras<sup>2</sup>

<sup>1</sup> Medical Image Processing and Analysis Group, Laboratory of Medical Physics,  
University of Patras, 26500 Patras, Greece.

e-mail: [mathan@upatras.gr](mailto:mathan@upatras.gr), web page: <http://mipa.med.upatras.gr>

<sup>2</sup> Medical Image and Signal Processing Laboratory, Department of Medical Instruments Technology,  
Technological Educational Institute of Athens, Athens 12210, Greece.

e-mail: [cavouras@teiath.gr](mailto:cavouras@teiath.gr), web page: <http://medisp.bme.teiath.gr>

<sup>3</sup> Medical Imaging Department, EUROMEDICA Medical Center, 2 Mesogeion Avenue, Athens, Greece

**Keywords:** wavelet, image enhancement, histogram equalization, mammography.

**Abstract.** *The purpose of this study was to investigate the effectiveness of five wavelet-based filters in enhancing mammograms. Wavelet-based image enhancement was implemented by processing the Discrete Wavelet Transform detail coefficients. In addition, the wavelet-based filters were comparatively evaluated against five conventional Histogram Equalization Filters. Histogram equalization enhancement was based on modifying the image contrast by adjusting the gray-level probability density function (uniform, exponential, rayleigh and two hyperbolic). These filters were applied to 130 digitized mammograms. The processed mammograms were blind-reviewed by an expert radiologist by means of eleven image quality parameters, including definition of masses, vessels and micro-calcifications. The wavelet-based filters enhanced significantly 6 of the evaluated parameters. On the other hand the two histogram equalization hyperbolic filters were found to effectively improve 7 parameters. The rest histogram equalization filters showed no significant image enhancement. Important results were the improved visualization of micro-calcifications and improvement of mammograms with fatty and fatty-granular content. Overall processing time was less than 3s for all filters on a typical desktop PC, rendering the application plausible for clinical routine.*

### 1 INTRODUCTION

Mammography is the most efficient technique used for the early detection of cancer and other diseases related to breast. According to recent epidemiology researches, one out of ten women is expected to suffer from breast cancer during her lifetime. Although early detection of breast cancer in most times leads to total treatment, however it is difficult to be diagnosed due to complicated breast structure<sup>[1]</sup>.

A variety of filters have been developed over the past few years for enhancing digital X-ray mammograms<sup>[6-8]</sup>. In the present study, a systematic evaluation of the performance of five wavelet-based filters was performed. Moreover, a comparative evaluation of the wavelet-based filters with five conventional histogram equalization filters was also carried out. Additionally, a novel non-linear wavelet-based filter is proposed, especially designed for enhancing digital mammograms. For the evaluation of the results, an experienced radiologist assessed 11 mammographic image quality parameters in all processed mammograms, in order to investigate the image-enhancing effectiveness of the filters. For that task, a custom made program, using C++ environment was developed.

### 2 MATERIALS AND METHODS

#### 2.1 Wavelet-Based Enhancement Filters

The wavelet-based enhancement procedure involves three steps<sup>[2, 3, 4]</sup>. First, the DAUB4 DWT (Discrete Wavelet Transform)<sup>[5]</sup> was applied in five scales for each mammogram. Second, the detail coefficients were processed in all scales<sup>[6,7,8,9,10, 11]</sup> and finally, the enhanced mammograms were obtained by using the inverse wavelet transform (IDWT)<sup>[5]</sup>. An example of 2-scale decomposition procedure is illustrated in figure 1.

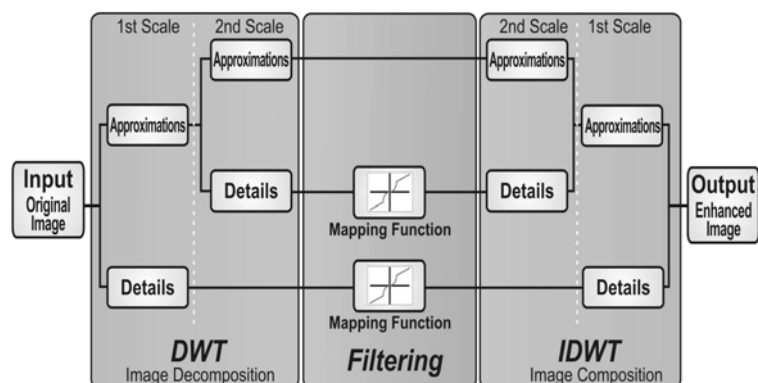


Figure 1. Basic scheme of 2-scale decomposition wavelet based filtering technique

### 2.1.1 Simple Piece-Wise Linear Mapping (SPWLMF) Function.

In SPWLMF, the multi-scale coefficients of the DWT are modified according to equation 1. An appropriate threshold value  $|T|$  as well as an amplification factor  $G$  are manually chosen by the physician. Schematically, the redistribution of the wavelet coefficients is illustrated in figure 2.

$$W_{out} = \begin{cases} W_{in} + T \cdot (G - 1) & \text{if } W_{in} > T \\ W_{in} - T \cdot (G - 1) & \text{if } W_{in} < -T \\ G \cdot W_{in} & \text{otherwise} \end{cases} \quad (1)$$

Where  $W_{out}$  denotes the output and  $W_{in}$  the input coefficient values of the Detail Matrix.  $T$  and  $G$  are threshold and gain values respectively.

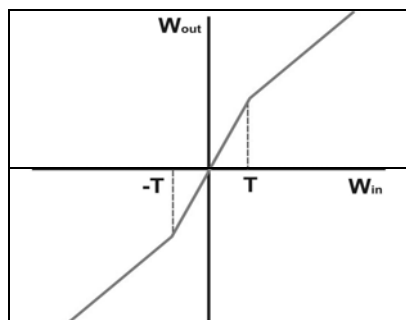


Figure 2: Simple Piece-Wise Linear Mapping Function ( $F1$ )

### 2.1.2 Hard-Threshold Function (HTF) Function.

In HTF, the modification process of the wavelet coefficients is similar to SPWLMF. The major difference is that the values between the thresholds  $|T|$  are neutralized. HTF is illustrated in equation 2 and figure 3 respectively.

$$W_{out} = \begin{cases} W_{in} + T \cdot (G - 1) & \text{if } W_{in} > T \\ W_{in} - T \cdot (G - 1) & \text{if } W_{in} < -T \\ 0 & \text{otherwise} \end{cases} \quad (2)$$

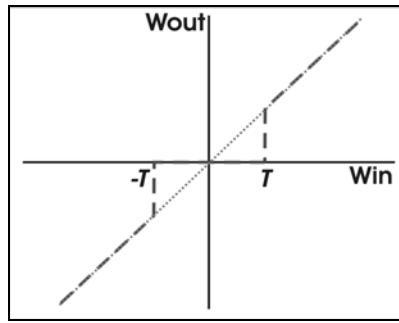


Figure 3: Hard-Threshold Function function (F2)

### 2.1.3 Wavelet Enhancement With Noise Suppression (WEWNS) Function.

According to WEWNS, two independent threshold values,  $|T_1|$  and  $|T_2|$ , are selected and the wavelet coefficients are processed using equation 3.

$$W_{out} = \begin{cases} W_{in} + T_2 \cdot (G-1) - T_1 \cdot G & \text{if } W_{in} > T_2 \\ G \cdot (W_{in} - T_1) & \text{if } T_1 < W_{in} \leq T_2 \\ 0 & \text{if } -T_1 \leq W_{in} \leq T_1 \\ G \cdot (W_{in} + T_1) & \text{if } -T_2 \leq W_{in} < -T_1 \\ W_{in} - T_2 \cdot (G-1) + T_1 \cdot G & \text{if } W_{in} < -T_2 \end{cases} \quad (3)$$

where,  $W_{out}$  denotes the output and  $W_{in}$  the input coefficient values of the detail wavelet coefficient matrix,  $G$  is the gain value, while  $T_1$  and  $T_2$  are two threshold values<sup>[3,4]</sup>.

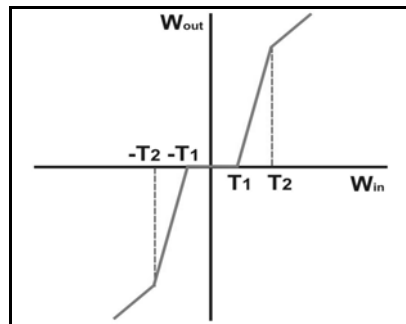


Figure 4: Wavelet Enhancement With Noise Suppression function (F3)

### 2.1.4 Sigmoidal non-Linear Enhancement (SNLEF) Function.

In SNLEF filter, wavelet coefficients laid between the threshold value  $|T|$ , are modified according to a sigmoid function illustrated in equation 4 and figure 5.

$$W_{out} = a \left[ \text{sigm}(G(W_{in} - T)) - \text{sigm}(-G(W_{in} + T)) \right]$$

$$a = \frac{1}{\text{sigm}(G(1 - T)) - \text{sigm}(-G(1 + T))} \quad (4)$$

$$\text{sigm}(y) = \frac{1}{1 + e^{-y}}$$

Where  $W_{out}$  denotes the output coefficients,  $W_{in}$  are the input coefficients and parameters  $T$  and  $G$  control the threshold and the gain respectively.

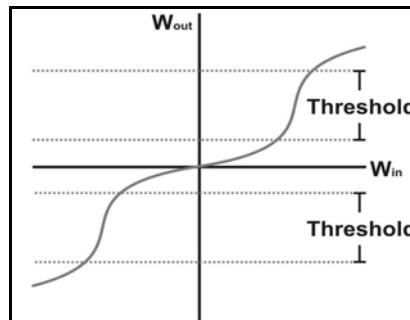


Figure 5: Sigmoidal non-Linear Enhancement Function (F4)

### 2.1.5 Non Linear Enhancement (NLEF) Function.

According to NLEF filter, wavelet coefficients between the threshold values  $/T/$  are squared, as illustrated in equation 5 and figure 6.

$$W_{out} = \begin{cases} W_{in} + T \cdot (1-T) & \text{if } W_{in} > T \\ W_{in} - T \cdot (1-T) & \text{if } W_{in} < -T \\ W_{in}^2 & \text{otherwise} \end{cases} \quad (5)$$

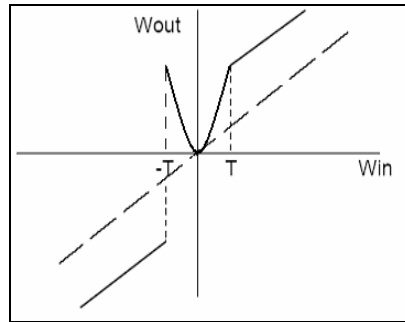


Figure 6: Non Linear Enhancement Function (F5)

## 2.2 Histogram Equalization Filters

Five Histogram Equalization Mapping Functions (HEMF) were also developed in C++ and applied to mammograms <sup>[1, 2, 3]</sup>. The HEMF functions are based on corresponding probability density models for the desired output graylevel histogram. Table 1 illustrates the equations that were used in this study.

OUTPUT PROBABILITY DENSITY MODELS		CORRESPONDING MAPPING FUNCTIONS
<b>Uniform (F6)</b>	$P_g(g) = \frac{1}{g_{\max} - g_{\min}}$	$g = (g_{\max} - g_{\min})CDF + g_{\min}$
<b>Exponential (F7)</b>	$P_g(g) = c \cdot \exp[-c(g - g_{\min})]$	$g = g_{\min} - \frac{1}{c} \ln(1 - CDF)$
<b>Rayleigh (F8)</b>	$P_g(g) = \frac{g - g_{\min}}{c^2} \exp\left[-\frac{(g - g_{\min})^2}{2c^2}\right]$	$g = g_{\min} + \left[2c^2 \ln\left(\frac{1}{1 - CDF}\right)\right]^{1/2}$
<b>Hyperbolic_1 (Cube Root) (F9)</b>	$P_g(g) = \frac{1}{3} \frac{g^{-2/3}}{g_{\max}^{1/3} - g_{\min}^{1/3}}$	$g = \left[(g_{\max}^{1/3} - g_{\min}^{1/3})CDF + g_{\min}^{1/3}\right]^3$
<b>Hyperbolic_2 (Logarithmic) (F10)</b>	$P_g(g) = \frac{1}{g[\ln(g_{\max}) - \ln(g_{\min})]}$	$g = g_{\min} \left[\frac{g_{\max}}{g_{\min}}\right]^{CDF}$

Table 1: The output probability density models and the respective mapping functions

where,  $g_{min}$  and  $g_{max}$  are the minimum and maximum gray-level values in the image,  $CDF$  is the Cumulative Distribution Function of the histogram,  $g$  is the calculated gray-tone of the processed image, and  $c$  is a weight factor.

### 2.3 Set up of the study

One hundred and thirty mammograms were obtained using a General Electric DMR Plus mammographic unit with molybdenum/molybdenum (Mo/Mo) anode/filter combination and 650mm focus to film distance (FFD). Film images were digitized on a Microtec Scanmaker II SP (1200x1200 dpi, 8-bit graylevel). These 130 mammograms were analyzed by a custom-developed software in C++. A number of mammogram image quality parameters were evaluated. Specifically, each filter was evaluated based on the choice of positive or negative effects related to:

1. The contrast between dark and light areas.
2. The improvement of normal fatty breasts.
3. The improvement of dense fibro-granular breasts.
4. The display quality and delineation of calcifications.
5. The good visualization of vessels, veins, ducts.
6. The good visualization of pathological findings.
7. Image detail related to the characterization of a lesion as benign or malignant.
8. The accentuation of tumor inhomogeneity.
9. The delineation of tumor borders.
10. The good visualization of breast skin and soft tissues.
11. The good visualization of the thoracic muscle.

## 3 RESULTS AND DISCUSSION

Image contrast is a significant parameter for the physicians in order to assess the nature of a tumor. In the case of dense breasts, assessment is difficult due to low contrast in the mammogram. Thus, increasing image contrast is essential for more accurate diagnosis. According to our results (see parameter 1 in Table 2), the five wavelet-based filters as well as the two hyperbolic filters managed to increase image contrast sufficiently in almost all of the cases. Percentage scores achieved by the enhancement filters in each evaluated parameter are illustrated in Table 2.

The structure of the breast is influenced by patient's age. In the case of young women with dense breast, mammograms appeared to be predominantly white. However, senior women, whose breasts consist of fatty tissue, mammograms appeared darker. In both patient groups, the wavelet-based filters and the two hyperbolic filters, managed to improve images satisfactorily (see parameters 2 and 3 in Table 2) while the rest of the filters failed to improve mammograms significantly.

One of the most important tasks in screening mammography is the identification and localization of micro-calcifications. Adequate visualization of micro-calcifications was achieved by the two hyperbolic histogram equalization filters and the exponential (see parameter 4 in Table 2). In contrast, better visualization of soft tissues, such as veins, vessels and ducts (see parameter 5 in Table 2) was attained by the wavelet-based filter.

Another important task for the characterization of a tumor as malignant or benign is considered to be the morphology, the boundaries and the textural structure of the tumor (see parameters 6, 7, 8 and 9 in Table 2). Sufficient delineation of the borders, as well as improvement of pathological findings was accomplished by the two hyperbolic filters followed by the exponential filter.

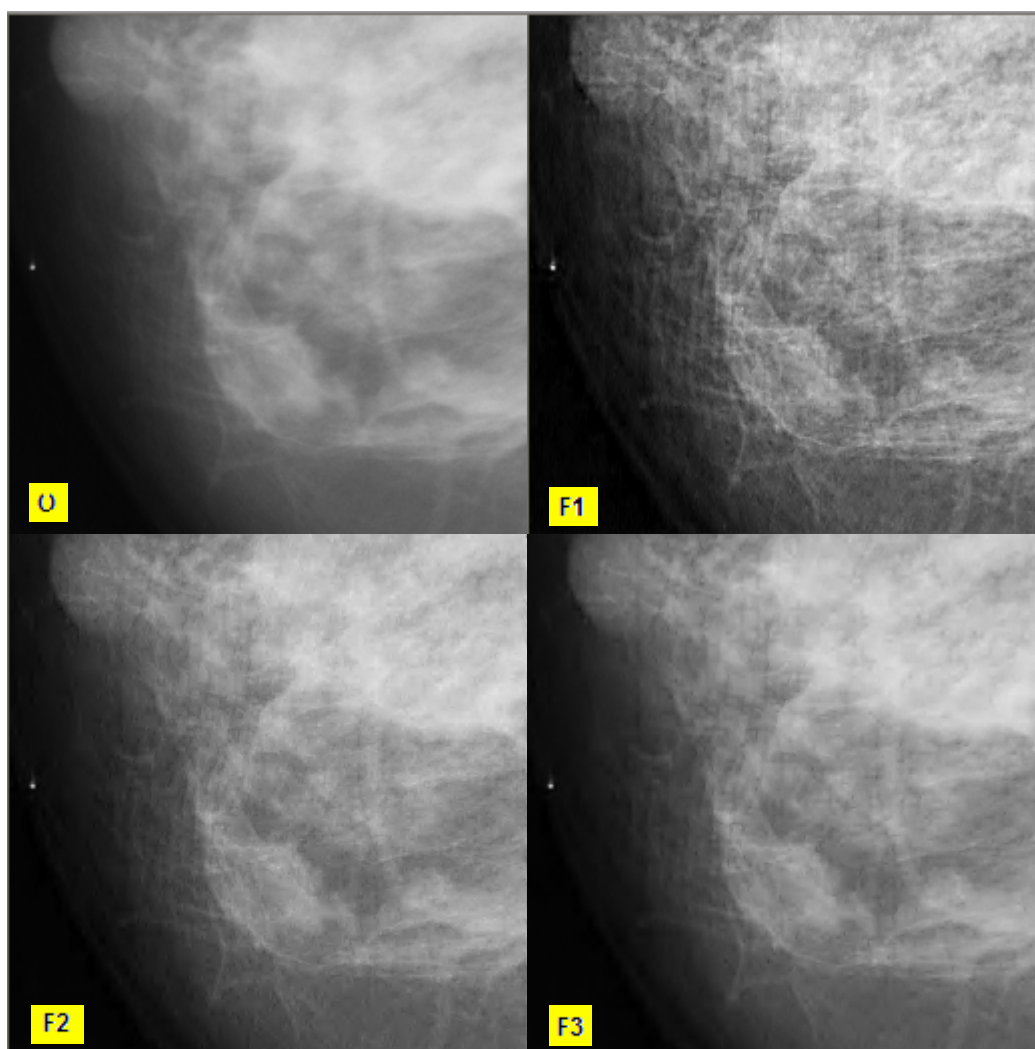
Parameters	F1	F2	F3	F4	F5	F6	F7	F8	F9	F10
1	58	71	71	69	95	1	38	3	68	91
2	58	63	63	52	95	0	33	1	67	88
3	18	29	29	29	95	0	36	2	67	90
4	2	4	4	4	7	0	21	0	24	24
5	22	36	36	36	38	0	1	0	2	8
6	8	9	9	9	10	0	23	2	30	39
7	10	12	12	12	15	0	26	0	34	40
8	8	8	8	8	9	0	26	0	30	35
9	10	12	12	12	12	0	26	1	36	47

<b>10</b>	50	55	55	55	60	14	0	0	3	0
<b>11</b>	46	48	48	48	66	0	0	0	0	1

Table 2: Percentage improvement achieved by each filter

Breast skin is directly related to infections of subcutaneous fat, sebaceous cysts, hematomas and dermal nevi (see parameter 10 in Table 2). Histogram equalization filters failed to enhance images. In contrast, wavelet-based filters succeeded in enhancing the mammograms in almost 50% of the cases. Finally, in the uncommon cases of retro-mammary space lesions or auxiliary lymphadenopathy findings, wavelet-based filters managed to improve images adequate, while the histogram equalization filters failed.

An example of a processed mammogram (Region Of Interest ROI) with all filters is illustrated in figures 7 and 8.



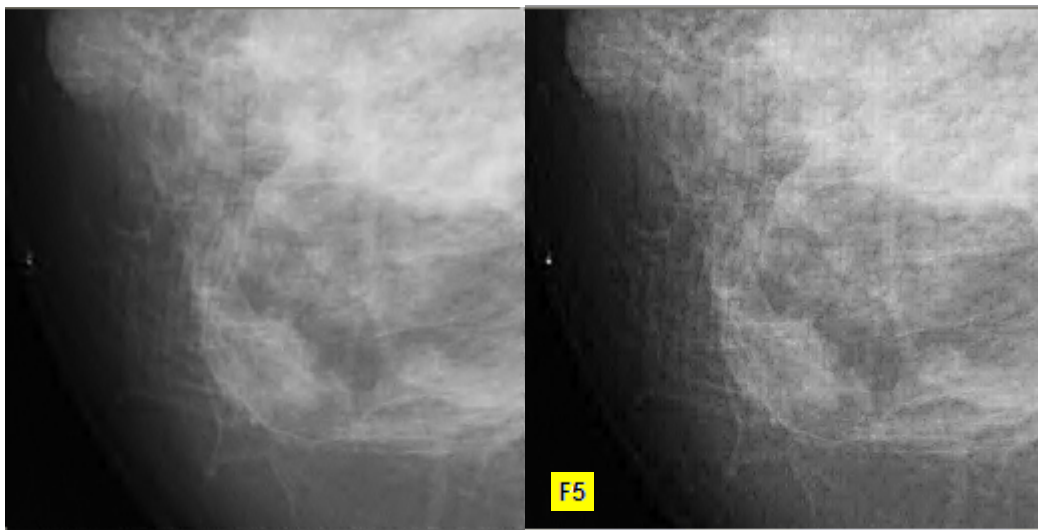
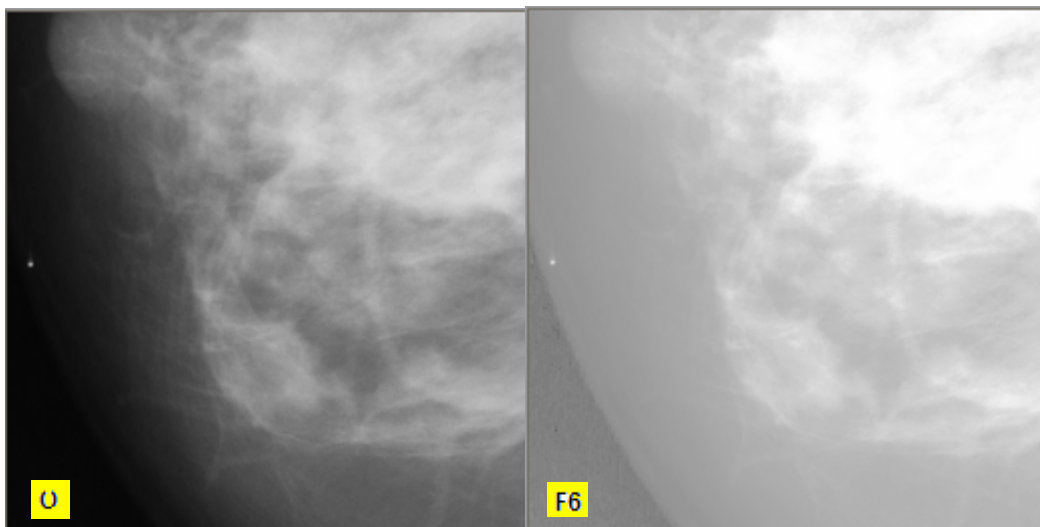


Figure 7: Original image (O) and 5 images processed by the wavelet filters (F1-F5).



F7

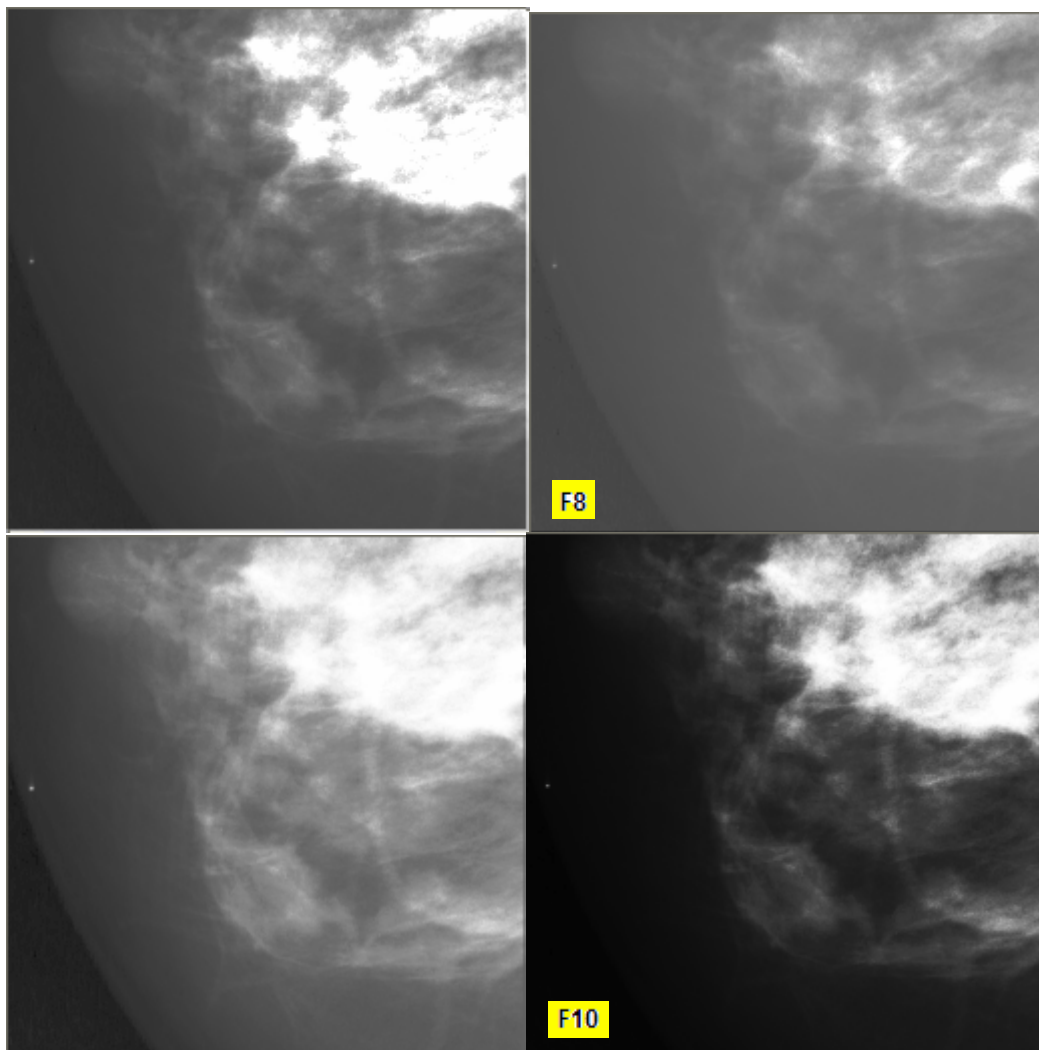


Figure 8: Original image (O) and 5 images processed by histogram the equalization filters (F6-F10)

#### 4 CONCLUSIONS

According to our results, it was found that the wavelet based techniques managed to accomplish better visualization of the breast skin, thoracic muscle, vessels, veins, and ducts, as well as to enhance the contrast of mammograms with normal fatty tissue. Significant improvement was also accomplished by the hyperbolic-1 and hyperbolic-2 (F9, F10) histogram equalization filters, in cases such as dense or fatty breasts. Hyperbolic filters also increased the overall contrast of the mammograms and contributed in the better visualization of tumors and micro-calcifications. Thus, the optimal choice for the proper filter is related to the specific application. Regarding all filters, processing time was less than 3sec, on a typical desktop PC (Intel Pentium4/ 2.4GHz, 512MB RAM), rendering them plausible for real clinical applications.



## REFERENCES

- [1] American Cancer Society <http://www.cancer.org>.
- [2] Pratt W. K. (1991): “Digital Image Processing”, 2<sup>nd</sup> Edition, John Wiley & Sons, New York, 275-285.
- [3] Gonzales R. C., Woods R. E. (1992): “Digital Image Processing”, Addison-Wesley, 167-190.
- [4] Weeks A. A. (1996): “Fundamentals of Electronic Image Processing”, Wiley-IEEE Press, 109-120.
- [5] Daubechies I. (1988): “Orthonormal Bases of Compactly Supported Wavelets”, *Communication of Pure and Applied Math.* 41 : 909-996.
- [6] Mekle R, Laine A., Smith S., Singer C., Koenigsberg T., Brown M. (2000): “Evaluation of a multiscale enhancement protocol for digital mammography”, *Wavelet Applications in Signal and Image Processing VIII, Proc. SPIE* vol. 4119, p. 1038-1049.
- [7] Brown T. J. (2000): “An adaptive strategy for wavelet based image enhancement”, *Proceeding of IMVIP 2000 - Irish Machine Vision and Image Processing Conference*, Dublin, Ireland, p. 67-81.
- [8] Brown T. J. (2001): “Differential Image Enhancement via Wavelet Foveation”, *Proceeding of IMVIP 2001- Irish Machine Vision and Image Processing Conference*, Dublin, Ireland, pp. 179-192.
- [9] Athanasiadis E., Piliouras N., Sidiropoulos K., Georgiou H., Makris C., Dimitropoulos N., Cavouras D. (2004), “Mammographic Image Enhancement using Wavelet-Based Processing and Histogram Equalization”, *1st International Conference “From Scientific Computing to Computational Engineering” (1st IC-SCCE)*, Athens, Greece.
- [10] Sidiropoulos K., Piliouras N., Athanasiadis E., Georgiou H., Makris Ch., Dimitropoulos N., Cavouras D. (2004), “Statistical Versus Wavelet-Based despeckling techniques for enhancing medical ultrasound images”, *1st International Conference “From Scientific Computing to Computational Engineering” (1st IC-SCCE)*, Athens, Greece.
- [11] Kefalas D., Athanasiadis E., Sidiropoulos K., Glotsos D., Dimitropoulos N., Cavouras D. (2005), “Wavelet based Mammographic Image Enhancement using an Operator Adaptive Non-Linear Enhancement Function”, *“1st International Conference on Experiments / Process / System Modeling / Simulation / Optimization – 1st IC-EpsMsO, Laboratory of Fluid Mechanics and Energy (LFME) of University of Patras*, Athens, Greece.